



OPEN ACCESS

EDITED BY

Yi Pan,
Hohai University, China

REVIEWED BY

Shuxue Liu,
Dalian University of Technology, China
Zhiyao Song,
Nanjing Normal University, China
Gang Wang,
Hohai University, China

*CORRESPONDENCE

Zijun Zhou
✉ charlebilly@163.com

SPECIALTY SECTION

This article was submitted to
Coastal Ocean Processes,
a section of the journal
Frontiers in Marine Science

RECEIVED 18 October 2022

ACCEPTED 09 December 2022

PUBLISHED 12 January 2023

CITATION

Zhou Z, Sun Z, Zhou Y, Zuo Q,
Wang H, Chen Y and Huang F (2023)
Laboratory study of the combined
wave and surge overtopping-induced
normal stress on dike.
Front. Mar. Sci. 9:1073345.
doi: 10.3389/fmars.2022.1073345

COPYRIGHT

© 2023 Zhou, Sun, Zhou, Zuo, Wang,
Chen and Huang. This is an open-
access article distributed under the
terms of the [Creative Commons
Attribution License \(CC BY\)](https://creativecommons.org/licenses/by/4.0/). The use,
distribution or reproduction in other
forums is permitted, provided the
original author(s) and the copyright
owner(s) are credited and that the
original publication in this journal is
cited, in accordance with accepted
academic practice. No use,
distribution or reproduction is
permitted which does not comply with
these terms.

Laboratory study of the combined wave and surge overtopping-induced normal stress on dike

Zijun Zhou^{1,2*}, Zhongbing Sun^{1,2}, Yiren Zhou^{1,2}, Qihua Zuo^{1,2},
Hongchuan Wang^{1,2}, Yongping Chen^{1,3} and Feiyang Huang^{1,3}

¹State Key Laboratory of Hydrology-Water Resources and Hydraulic Engineering, Nanjing Hydraulic Research Institute, Nanjing, China, ²Nanjing Hydraulic Research Institute, Nanjing, China, ³College of Harbor, Coastal and Offshore Engineering, Hohai University, Nanjing, China

Normal stress on dikes is one of the most critical parameters for a sound dike design. With more rapidly rising sea levels due to global warming, dikes are seriously threatened by overtopping induced by the combination of wave and storm surge. Compared with wave overtopping on positive freeboard, the curling breaking wave on dikes induced by the combined wave and surge overtopping may destroy the weakly protected dike crest and landward slope. Thus, in order to prevent severe damage to dikes, it is necessary to fully understand the normal stress induced by the combined wave and surge overtopping. In this paper, physical model tests were carried out to study the normal stress on dike induced by the combined wave and surge overtopping. Two characteristics of normal stress on dike were observed. The spatial distribution of normal stress on dike was also analyzed. It was found that the Weibull distribution can be used to effectively describe the statistical distribution of peak normal stresses. Furthermore, by curve fitting of the laboratory measured data, the Weibull factors on the part of the crest and the upper part of the landward slope were obtained.

KEYWORDS

dike, combined wave and surge overtopping, normal stress, weibull distribution, physical model

1 Introduction

The normal stress on dikes is one of the most critical parameters in their design. In conventional dikes, the dike crest is normally higher than the sea level (positive freeboard), and the seaward slope is also well protected with an armor layer and is able to withstand strong wave impacts. Several previous studies have focused on the normal stress (wave pressure) induced by waves on the seaward slope under positive

freeboard (e.g., Hattori et al., 1994; Jensen et al., 2014; Zhou et al., 2020; Celi et al., 2021; Pan et al., 2022; Raby et al., 2022). These studies found that the large value of normal stress often occurs when the breaking wave swashes directly against the seaward slope (Hattori et al., 1994).

With more rapidly rising sea levels due to global warming (IPCC, 2012), there is a serious threat to dikes induced by the combined wave and surge overtopping (i.e., wave overtopping under negative freeboard) (Hughes, 2008). For example, during Hurricane Katrina in 2005, the combined wave and surge overtopping caused more than 50 breaches of dikes in New Orleans (ASCE Hurricane Katrina External Review Panel, 2007). Compared with the threat induced by wave overtopping on positive freeboard, the curling breaking wave on dikes induced by the combined wave and surge overtopping may cause more severe damage on the less protected, vulnerable dike crest and landward slope, although they are paved with grass or gravel.

After Hurricane Katrina, many hydraulic parameters, such as the average overtopping discharge, the individual wave overtopping volumes, flow velocity, flow thickness, turbulent kinetic energy, and the shear stress of the combined wave and surge overtopping, have been investigated and thoroughly studied (e.g., Reeve et al., 2008; Hughes and Nadal, 2009; Hughes and Nadal, 2009; Hughes et al., 2011; Li et al., 2012; Pan et al., 2012; Pan et al., 2013a; Pan et al., 2013b; Yuan et al., 2014; Pan et al., 2015; EurOtop, 2017; Pan et al., 2020). Despite this, the normal stress on the dike crest and the landward slope has been seldom discussed and is still not well understood. This is because, under a high value of negative freeboard, the overtopping flow of the combined wave and surge is similar to the surge-only overflow, which passes the dike crest smoothly and causes high shear stress along the dike, the normal stress being small enough to be neglected. However, under a lower value of negative freeboard (Pan et al., 2020), the overtopping

flow of the combined wave and surge is similar to the wave-only overtopping flow. The curling breaking wave may be generated and swashed downward directly against the dike crest or on the landward slope. In this case, a large normal stress is exerted on the dike crest or on the landward slope. Consequently, neglecting this extra normal stress in the design of dikes may potentially compromise the dike stability or cause dike breaching. Therefore, the study of the normal stress on dikes induced by the combined wave and surge overtopping is essential.

In this paper, physical model tests were conducted to investigate the normal stress on dike induced by the combined wave and surge overtopping. At the same time, the average overtopping discharges were accurately measured and compared with those from several existing theoretical and experimental formulas. From the measured time series of the normal stresses on dike, two characteristics (i.e., abrupt and gradual change) were observed. These were consonant with the two wave passing patterns (i.e., breaking or smooth passing). Furthermore, the spatial distribution of the normal stress on dike was analyzed. The statistical distribution of the peak normal stress was effectively expressed by the Weibull distribution. Additionally, the Weibull factors, respectively on the dike crest and on the upper part of the landward slope, were calculated by curve fitting of the laboratory measured data.

2 Laboratory experiment setup

Physical model tests were carried out in the wave flume (175 m long, 1.8 m wide, and 1.8 m deep) at the River and Harbor Engineering Department of Nanjing Hydraulic Research Institute, China (Figure 1). The wave flume was equipped with a blade-type wave maker.



FIGURE 1
Photo of the wave flume.

A trapezoidal dike cross-section was designed with a geometry scale of 1:10 normal model. The whole layout of the experiment is shown in Figure 2. A long 1:100 approach slope, following a 1:10 transition slope, was connected to the bottom of the flume in the front of the model. The distance between the tested dike cross-section to the wave maker was 42.0 m. The crest of the tested dike cross-section was 0.925 m above the bottom of the wave flume (0.325 m above the top of the 1:10 slope), while the width of the dike crest was 0.257 m in model scale. The seaward slope of the dike model section was 1:4.25, while the landward slope was 1:3. Three plastic plates were respectively installed on the seaward slope, the crest, and the landward slope. The bottom of the flume was equipped with a bidirectional circulating pump, which was used to provide a return flow in order to counterbalance the mean overtopping due to the combined wave and surge, as shown in Figure 2.

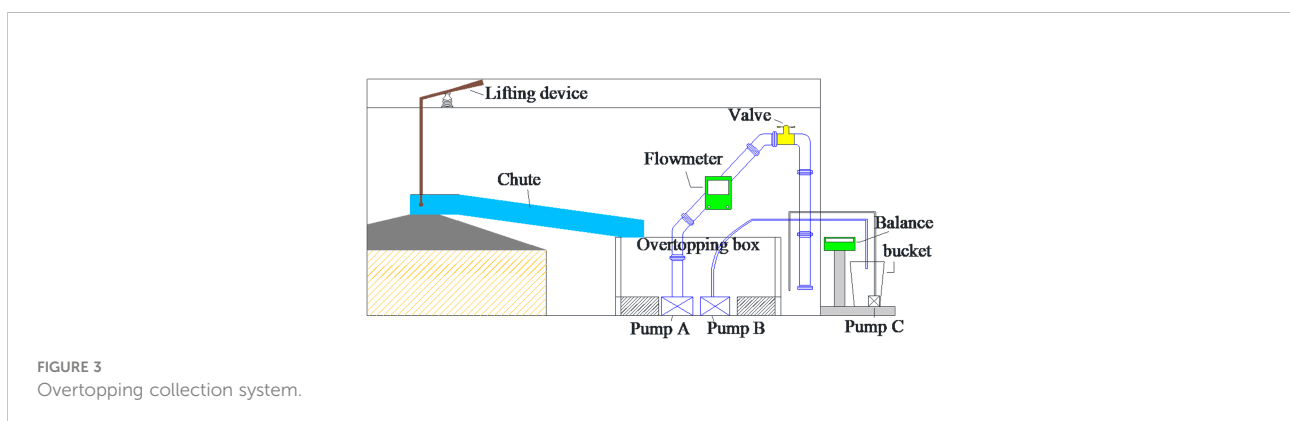
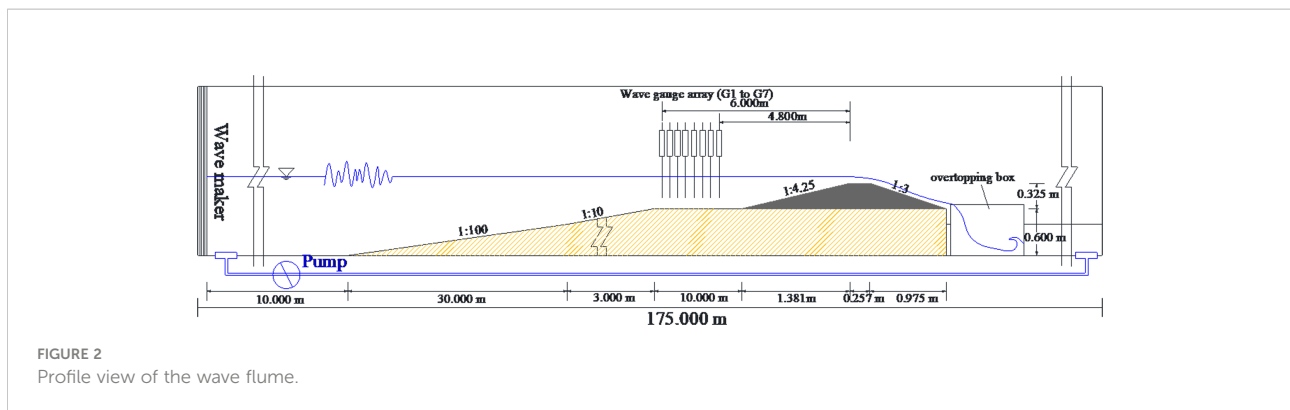
Seven wave gauges, G1–G7, were placed near the toe of the seaward slope (Figure 2). From the measured time series of wave heights, the incident and reflected wave heights were calculated via a three-point method. The measuring frequency of the wave gauge was 100 Hz.

The average overtopping discharge was measured at the inside of the tested section by collecting the overtopping water (over a width of 0.1 m) via an overtopping chute (a lifting device was installed in the front of the chute, which enables placing and

removing the chute from the dike crest quickly) into the overtopping box (equipped with two large pumps). A larger pump (pump A) was connected with a Φ10-cm steel pipe to the back of the wave flume, and a flow meter was placed on the steel pipe. A smaller pump (pump B) was connected with a plastic pipe to a bucket that is constantly weighed on a balance. Pump C was used to pump the water from the bucket to the wave flume in order to keep the water level unchanged in the wave flume during the test (see Figure 3).

At the beginning of the test, the chute was lifted under the surge-only overflow condition. When the wave reached the dike, the chute was placed down on the dike crest and timing was started. In smaller discharge test cases ($R_c > -0.06$ m), pump B was used to pump the water from the overtopping box into the bucket and then a balance was used to weigh the water. In larger discharge test cases ($R_c \leq -0.06$ m), pump A was opened and a flow meter was used to measure the discharge. At the end of wave making, we lifted the chute and stopped timing to measure the total water volume or the discharge during this period. Using this process, the average discharge was obtained.

As shown in Figure 4, the normal stress on the dike was measured by 15 pressure gauges, P1–P15, of which five were evenly distributed on the dike crest (the interval was 0.043 m in model scale) and 10 were located on the landward slope (the interval was 0.075 m in model scale). The measuring frequency



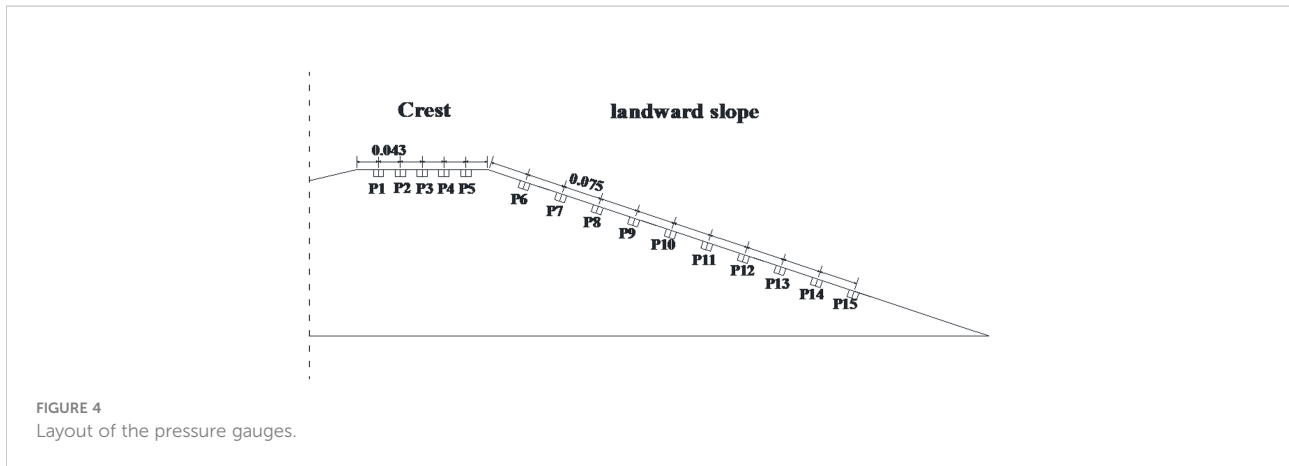


FIGURE 4
Layout of the pressure gauges.

of the pressure gauge was 100 Hz. The collected pressure data were filtered to remove unwanted higher- or lower-frequency oscillations.

In this test, the incident waves were generated according to the JONSWAP (Joint North Sea Wave Project) spectrum. A total of 15 unique wave conditions are listed in Table 1. Each test lasted for 480 s. This gave about 140 waves for tests with the longest peak wave periods.

3 Average discharge of the combination of wave and surge

Understanding the average discharge is the first step to understanding the normal stresses on dikes induced by the combined wave and surge overtopping. In this section, the measured average discharge in the test was compared with those of the existing average discharge formulas.

TABLE 1 Test cases of the physical model tests.

Test cases	Prototype-scale parameters		
	R_c (m)	H_{m0} (m)	T_p (s)
Trial 11	-0.30	1.03	4.11
Trial 12	-0.30	1.05	4.74
Trial 13	-0.30	1.03	6.32
Trial 14	-0.30	1.05	9.49
Trial 15	-0.30	1.37	4.74
Trial 21	-0.60	1.04	4.11
Trial 22	-0.60	1.08	4.74
Trial 23	-0.60	1.02	6.32
Trial 24	-0.60	1.05	9.49
Trial 25	-0.60	1.51	4.74
Trial 31	-0.90	1.00	4.11
Trial 32	-0.90	0.98	4.74
Trial 33	-0.90	0.97	6.32
Trial 34	-0.90	1.05	9.49
Trial 35	-0.90	1.52	4.74

R_c , freeboard; H_{m0} , wave height; T_p , wave period.

3.1 Existing average discharge formulas of the combination of wave and surge

Several formulas had been obtained from previous studies to estimate the average discharge of the combined wave and surge overtopping (e.g., [Reeve et al., 2008](#); [Hughes and Nadal, 2009](#); [EurOtop, 2017](#)).

In [EurOtop \(2017\)](#), the average overtopping discharge of the combined wave and surge overtopping can be calculated as:

$$q_{ws} = q_s + q_w \tag{1}$$

The average discharge was divided into two parts: surge-only overflow (q_s) and wave overtopping (q_w) with zero freeboard. The surge-only overflow (q_s) part was calculated as follows (e.g., [Henderson, 1966](#)):

$$q_s = \left(\frac{2}{3}\right)^{3/2} \sqrt{g} h_1^{3/2} \tag{2}$$

where g is the gravity acceleration and $h_1 (-R_c)$ is the upstream head.

The wave overtopping (q_w) part was calculated as follows (e.g., [Schüttrumpf et al., 2001](#)):

$$\frac{q_w}{\sqrt{gH_{m0}^3}} = 0.0537 \xi_{m-1,0} \xi_{m-1,0 < 2.0} \tag{3}$$

$$\frac{q_w}{\sqrt{gH_{m0}^3}} = \left(0.0136 - \frac{0.226}{\xi_{m-1,0}^3}\right) \xi_{m-1,0 > 2.0} \tag{4}$$

where H_{m0} is the significant wave height based on the wave spectrum and $\xi_{m-1,0}$ is the breaking parameter based on the deepwater wavelength and mean energy period. It should be noted that Eqs. 3, 4 show no relationship with relative freeboard because they are only applicable for cases with zero freeboard.

In [Reeve et al. \(2008\)](#), the average overtopping discharge formula was obtained using a numerical wave flume model, which can be calculated as:

$$Q_R = \frac{q_{ws}}{\sqrt{gH_s^3}} \frac{\sqrt{\tan \alpha}}{\xi_p} = 0.051 \exp\left(-1.98 \frac{R_c}{H_s \xi_p}\right) \text{ for breaking waves} \tag{5}$$

$$Q_R = \frac{q_{ws}}{\sqrt{gH_s^3}} = 0.233 \exp\left(-1.29 \frac{R_c}{H_s}\right) \text{ for non-breaking waves} \tag{6}$$

where ξ_p is the breaking parameter based on the deep-water wavelength and peak energy period. The value of freeboard (R_c) should be entered as a negative number.

In [Hughes and Nadal \(2009\)](#), the average overtopping discharge formula was obtained by a laboratory study on a wave flume with a prototype-to-model length scale of 25:1. The formula related to the dimensionless overtopping discharge and the relative freeboard can be described as:

$$\frac{q_{ws}}{\sqrt{gH_{m0}^3}} = 0.034 + 0.53 \left(\frac{-R_c}{H_{m0}}\right)^{1.58} \tag{7}$$

It should be noted that the wave period is not related to the average overtopping discharge, according to the conclusion of [Hughes and Nadal \(2009\)](#).

3.2 Analysis of the average overtopping discharge

[Table 2](#) lists the average overtopping discharge values measured in this test. [Figure 5](#) shows the dimensionless average discharge *versus* the relative freeboard for all 15 tests. The calculation results using the formulas of [EurOtop \(2017\)](#), [Reeve et al. \(2008\)](#), and [Hughes and Nadal \(2009\)](#) are also compared in [Figure 5](#). The fitting curve of the [Hughes and Nadal \(2009\)](#) formula (Eq. 7) is shown in [Figure 5](#). The data points calculated using the formulas of [EurOtop \(2017\)](#) (Eq. 1) and [Reeve et al. \(2008\)](#) (Eqs. 5, 6) were based on the wave conditions in this test.

As shown in [Figure 5](#), the data points from the tests were consistent with the calculation results of the formula of [EurOtop \(2017\)](#) in cases of very low absolute values of negative relative freeboard ($-0.4 \leq R_c/H_{m0} < 0$) and showed good fit with the formula of [Hughes and Nadal \(2009\)](#) in cases of higher absolute values of negative relative freeboard ($R_c/H_{m0} < -0.4$). However, all of the data points from the tests were smaller than those of the method of [Reeve et al. \(2008\)](#).

[Li et al., 2012](#) concluded that the relative freeboard reflects the proportional relationship between the surge-only overflow and the wave-only overtopping in the combination of surge and wave. [Figure 6](#) shows the ratio of q_{ws}/q_s *versus* the relative negative freeboard. For higher absolute values of relative freeboard, the average discharge of the combined wave and surge overtopping (q_{ws}) was almost equal to the discharge of the surge-only overflow (q_s). This indicates that the hydraulic parameters such as wave period and gradient of seaward slope may not be related to the average overtopping discharge under higher absolute values of negative relative freeboard. However, these hydraulic parameters were still considered in Eq. 1 [EurOtop, 2017](#)), whose estimates were larger under higher absolute values of relative freeboard.

On the other hand, for lower absolute values of relative freeboard, the average overtopping discharge of the combined wave and surge overtopping (q_{ws}) was slightly bigger than that of the surge-only overflow discharge (q_s). This indicates that, when the relative freeboard approaches zero, the wave is more influential in the average discharge of the combined wave and surge overtopping. Thus, the hydraulic parameters such as wave period and gradient of seaward slope still have obvious influences on the discharge under lower absolute values of negative relative freeboard. However, these hydraulic

TABLE 2 Measured average overtopping discharge.

Test cases	Hydraulic parameters		Average discharge	
	H_{m0} (m)	T_p (s)	q_s (m ³ /s/m)	q_{ws} (m ³ /s/m)
Freeboard: $R_c = -0.3$ m				
Trial 11	1.03	4.11	0.280	0.418
Trial 12	1.05	4.74	0.280	0.455
Trial 13	1.03	6.32	0.280	0.475
Trial 14	1.05	9.49	0.280	0.503
Trial 15	1.37	4.74	0.280	0.598
Freeboard: $R_c = -0.6$ m				
Trial 21	1.04	4.11	0.792	0.847
Trial 22	1.08	4.74	0.792	0.849
Trial 23	1.02	6.32	0.792	0.871
Trial 24	1.05	9.49	0.792	0.897
Trial 25	1.51	4.74	0.792	0.952
Freeboard: $R_c = -0.9$ m				
Trial 31	1.00	4.11	1.454	1.449
Trial 32	0.98	4.74	1.454	1.443
Trial 33	0.97	6.32	1.454	1.422
Trial 34	1.05	9.49	1.454	1.459
Trial 35	1.52	4.74	1.454	1.470

R_c , freeboard; H_{m0} , wave height; T_p , wave period; q_s , surge-only overflow; q_{ws} , wave overtopping.

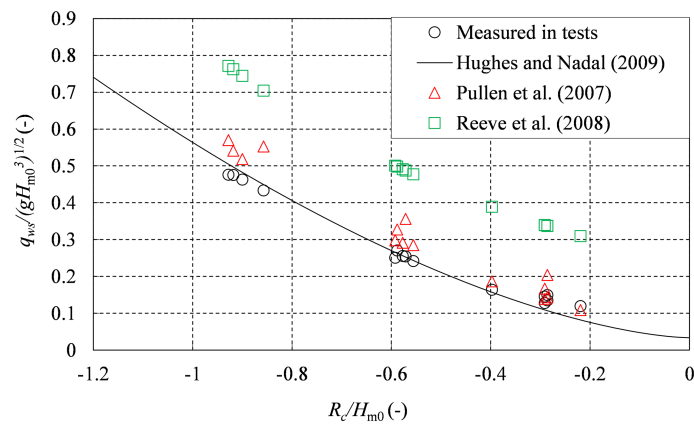


FIGURE 5 Dimensionless average discharge versus relative freeboard.

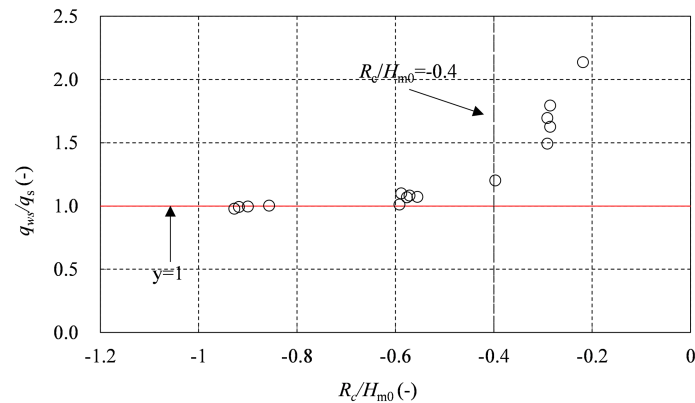


FIGURE 6
 q_{ws}/q_s versus the relative negative freeboard.

parameters were neglected in the formula of Hughes and Nadal (2009), which led to the unsatisfactory performance of Eq. 7 (Hughes and Nadal, 2009) in cases of lower absolute values of negative relative freeboard ($-0.4 \leq R_c/H_{m0} < 0$).

Therefore, Eq. 7 (Hughes and Nadal, 2009) can be used to calculate the average discharge of the combined wave and surge overtopping in cases of higher absolute values of negative relative freeboard ($R_c/H_{m0} < -0.4$), while Eq. 1 (EurOtop, 2017) can be used to calculate the average discharge of the combined wave and surge overtopping in cases of lower absolute values of negative relative freeboard ($-0.4 \leq R_c/H_{m0} < 0$).

4 Normal stress

This section analyzes the characteristic and spatial distributions of normal stress on the dike induced by the combined wave and surge overtopping. The Weibull distribution was used to represent the statistical distribution of peak normal stress.

4.1 Time series analysis

The time series of normal stress measured using a pressure gauge was used to analyze the characteristics of normal stress along the dike. Figure 7 gives two examples of the time series of normal stress measured by pressure gauge P1 on the front of the dike crest from trial 13 ($R_c = -0.3$ m, $H_{m0} = 1.03$ m, $T_p = 6.32$ s) and trial 33 ($R_c = -0.9$ m, $H_{m0} = 0.97$ m, $T_p = 6.32$ s). The values have been converted to the prototype scale according to a length scale of 10. Figure 7A displays the sharp increase of the normal stress at about 709, 734, and 742 s (as circled in Figure 8A), and much greater than that induced by the surge-only overflow (blue line). The sharp increase of normal stress (referred to as abrupt

change) indicates that the dike withstands an impulsive downward-flushing flow directly. As shown in Figure 7B, the normal stress increased slowly (referred to as gradual change), which is the order of the static pressure due to the wave elevation. As Pan et al. (2015) pointed out, breaking passing (plunging breaks on the crest or the landward slope) and smooth passing (waves passing without a breaker) of waves are the two passing patterns in the combination of wave and surge. In cases of lower absolute values of negative freeboard ($R_c = -0.3$ m), the main wave passing pattern is breaking passing, with the downward-flushing flow directly impacting the dike crest and the upper part of the landward slope and the normal stress characterized by abrupt change. In cases of medium absolute values of negative freeboard ($R_c = -0.6$ m), both wave passing patterns are possible, with the downward-flushing flow mainly impacting the upper part of the landward slope, the normal stress on the dike crest characterized by gradual change, and the normal stress on the upper part of the landward slope characterized by abrupt change. In cases of higher absolute values of negative freeboard ($R_c = -0.9$ m), the main wave passing pattern was smooth passing, and the normal stress on the dike was characterized by gradual change.

4.2 Spatial distribution of normal stress

Figure 8 shows six examples of the spatial distribution of 1% relative normal stress, $p_{1\%}^*$ (since the number of waves in this test was about 140, 1% normal stress can be regarded as the maximum value), along the dike with different values of freeboard (R_c), wave height (H_{m0}), and wave period (T_p). The dimensionless parameter 1% relative normal stress, $p_{1\%}^*$ ($p_{1\%}$ denotes that the normal stress level exceeds by 1% of the measured normal stress time series), in this figure is defined as $p_{1\%}^* = p_{1\%}/\gamma H_{m0}$, where γ is the water-specific weight, B is the

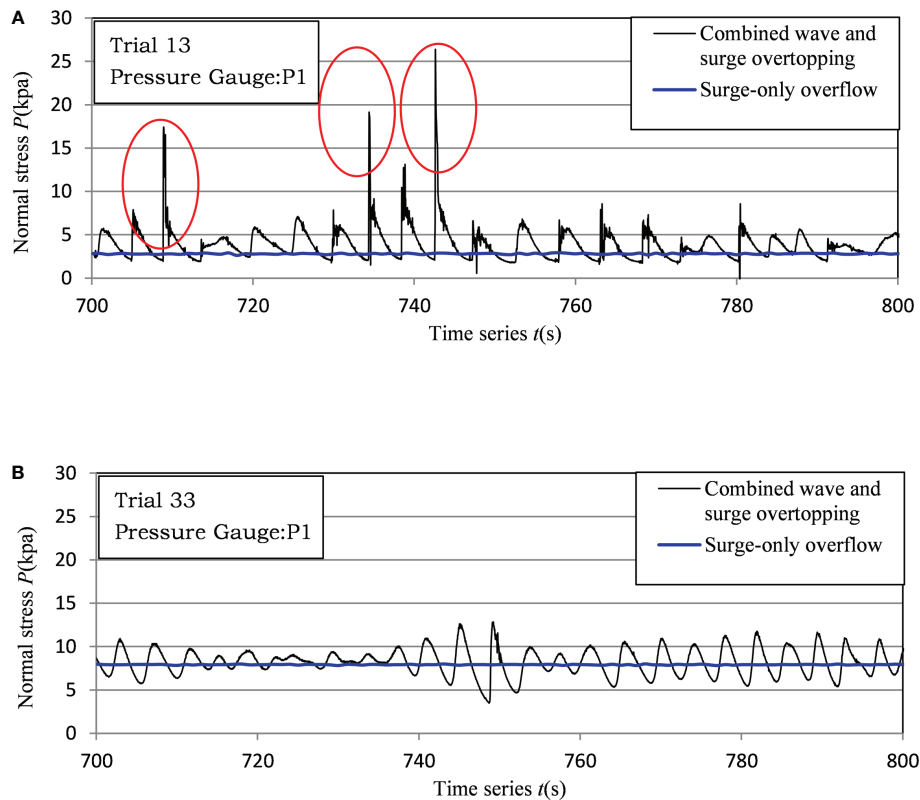


FIGURE 7
Samples of normal stresses time series at P1 on the dike crest: (A) abruptly change; (B) gradually change.

width of the dike crest, and x is the projection length of the measuring point on the horizontal line (see Figure 9).

It can be seen from Figures 8A, B that, under cases of lower absolute values of negative freeboard ($R_c = -0.3$ m), the 1% relative normal stress ($p_{1\%}^*$) on the dike crest ($0 \leq x/B < 1$) was large ($p_{1\%}^*$ was approximately 3). The maximum normal stress at different measurement points changed significantly, and the location where the maximum normal stress occurred moved back along the dike crest with the wave period increase. Obviously, the $p_{1\%}^*$ on the upper part of the landward slope ($1 \leq x/B < 2.1$) was large ($p_{1\%}^*$ was approximately 2–3), with the maximum normal stress increasing significantly with the increase of the wave period and the location where the maximum normal stress generally occurring at pressure gauges P7–P9 ($1.5 < x/B < 2.1$). The $p_{1\%}^*$ on the lower part of the landward slope ($x/B \geq 2.1$) was smaller and gradually decreased along the landward slope.

It is also apparent from Figures 8C, D that, in cases of medium absolute values of negative freeboard ($R_c = -0.6$ m), the $p_{1\%}^*$ on the dike crest ($0 \leq x/B < 1$) was relatively small ($p_{1\%}^*$ was approximately 2). The maximum normal stress at different measurement points changed little. The $p_{1\%}^*$ on the upper part of the landward slope ($1 \leq x/B < 2.1$) was larger than that

on the dike crest ($p_{1\%}^*$ was approximately 2.5), with the maximum normal stress increasing slightly with the increase of the wave period and the location where the maximum normal stress generally occurring at pressure gauges P7–P9 ($1.5 < x/B < 2.1$). The $p_{1\%}^*$ on the lower part of the landward slope ($x/B \geq 2.1$) was smaller and gradually decreased along the landward slope.

Finally, Figures 8E, F show that, in cases of higher absolute values of negative freeboard ($R_c = -0.9$ m), the spatial distribution trend of the normal stress along the dike was similar to that of the surge-only overflow, the $p_{1\%}^*$ being relatively small and the maximum normal stress occurring at the dike crest. According to the findings detailed in Section 4.1, normal stress was caused by the static pressure under higher absolute values of negative freeboard; thus, the normal stress on the dike crest increased slightly due to the larger wave height (Figure 8F), and there was no obvious correspondence with the wave period.

In summary, in the combined wave and surge overtopping, the normal stress caused by the downward-flushing flow impact under lower absolute values of negative freeboard was larger than that caused by the static pressure along the dike due to the wave elevation under higher absolute values of negative

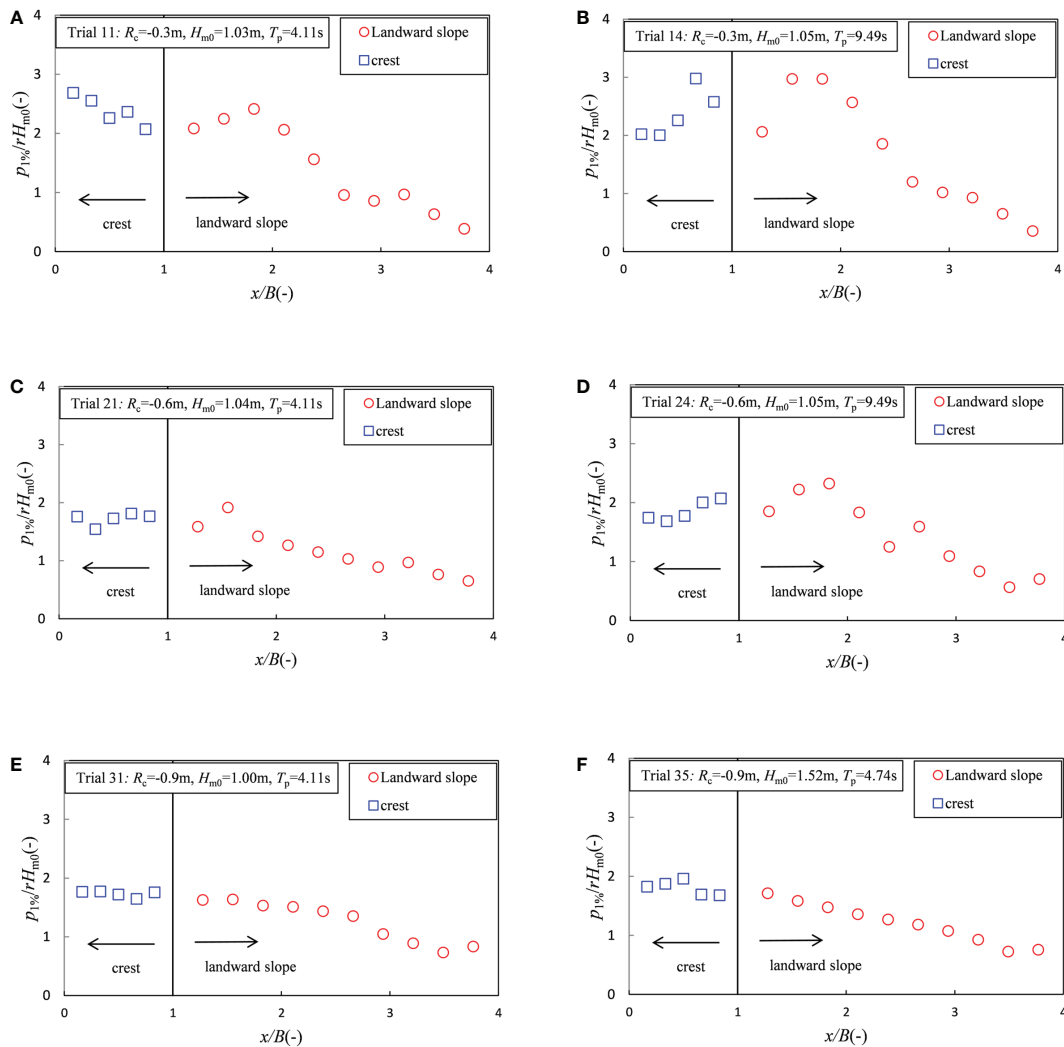


FIGURE 8 Spatial distribution of the relative normal stress along the dike. (A) Small wave period ($R_c = -0.3\text{m}$). (B) Large wave period ($R_c = -0.3\text{m}$). (C) Small wave period ($R_c = -0.6\text{m}$). (D) Large wave period ($R_c = -0.6\text{m}$). (E) Small wave height ($R_c = -0.9\text{m}$). (F) Large wave height ($R_c = -0.9\text{m}$).

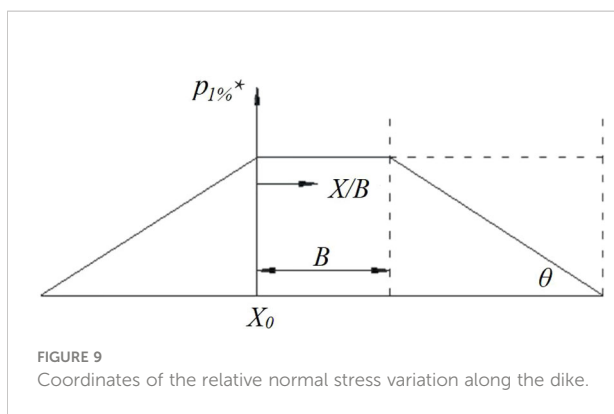


FIGURE 9 Coordinates of the relative normal stress variation along the dike.

freeboard. Moreover, the normal stress occurring at the dike crest ($0 \leq x/B < 1$) and the upper part of the landward slope ($1 \leq x/B < 2.1$) was larger than that at the lower part of the landward slope ($x/B \geq 2.1$).

4.3 Statistical distribution of normal stress

The values obtained from statistical distribution can be used for the probabilistic calculations of structures. In the present analysis, the two-parameter Weibull distribution was proposed to represent the statistical distribution of the peak value of relative normal stress ($p^* = p/\gamma H_{m0}$) measured by all the pressure gauges (P1–P15). The distribution can be written as follows:

$$P_{p^*} = P(p_i^* \leq p^*) = 1 - \exp\left[-\left(\frac{p^*}{a_p}\right)^{b_p}\right] \quad (8)$$

where P_{p^*} is the probability of the peak value of the relative normal stress per wave p_i^* being less than or equal to p^* , a_p is the scale factor, and b_p is the shape factor.

The findings in Sections 4.1 and 4.2 indicate that the normal stress induced by the combination of wave and surge overtopping expresses different characteristics (an abrupt or gradual change) on the dike crest and the upper and lower parts of the landward slope, thus, three examples of the Weibull distribution of the peak relative normal stress (semi-logarithmic ordinate) on the dike crest. The upper and lower parts of the landward slope are shown in Figure 10. Figure 10A shows an example of a mediocre fit from trial 21 ($R_c = -0.6$ m, $H_{m0} = 1.05$ m, $T_p = 9.49$ s) measured by pressure gauge P2 on the dike crest. Figure 10B shows an example of a good fit from trial 11 ($R_c = -0.3$ m, $H_{m0} = 1.00$ m, $T_p = 4.11$ s) measured by pressure gauge P7 on the upper part of the landward slope. Figure 10C shows an example of a poor fit from trial 21 ($R_c = -0.6$ m, $H_{m0} = 1.04$ m, $T_p = 4.11$ s) measured by pressure gauge P14 on the lower part of the landward slope.

In general, the fitting degrees between the test data measured by pressure gauges P1–P9 (dike crest and upper part of the landward slope) and the Weibull distribution were between the two cases shown in Figures 10A, B. Figure 10C shows that the fitting degrees between the test data measured by pressure gauges P10–P15 (lower part of the landward slope) and the Weibull distribution were poor. This is due to the fact that the flow thickness along the lower part of the landward slope was very small, and the normal stress caused by the static pressure was also very small. When the peak relative normal stress (p_i^*) becomes too small, the Weibull distribution may no longer be applicable. It should be mentioned that the determination of the maximum value of normal stress required for the stability of the structure is key to the dike design. The findings in Section 4.2 show that the normal stress occurring at the dike crest and the upper part of landward slope was obviously larger than that at the lower part of the landward slope; thus, this paper mainly focused on the normal stress on the dike crest and the upper part of the landward slope induced by the combined wave and surge overtopping.

The plots revealed that the freeboard (R_c), wave height (H_{m0}), and the wave period (T_p) closely controlled the scale of the cumulative probability distribution and were also closely related to the average overtopping discharge (q_{ws}). Figure 11 plots the scale factors a_{pc} on the dike crest and a_{ps} on the upper part of the landward slope versus the dimensionless overtopping discharge $[q_{ws}/m0_3^{*0.5}]$.

It can be seen from Figure 11A that, with the increase of $q_{ws}/m0_3^{*0.5}$, the scale factor a_{pc} on the dike crest first decreased slightly and then remained stable. This may be explained by the fact that the scale factor a_{pc} reflects the values of the average peak

relative normal stress; when the $q_{ws}/m0_3^{*0.5}$ is relatively small, with most of the waves passing the dike crest with a breaking passing pattern, the average peak normal stress is relatively large, which gives larger a_{pc} values. A comparison of pressure gauges P1–P5 indicated that the values of a_{pc} had no apparent regularity during each test case. The solid line is a best-fit empirical equation for the datasets given by the following equation:

$$a_{pc} = 78.6 \exp\left(-35.5 \frac{q_{ws}}{(gH_{m0}^3)^{0.5}}\right) + 1.36 \quad (9)$$

It can be seen from Figure 11B that, with the increase of $q_{ws}/m0_3^{*0.5}$, the scale factor a_{ps} on the upper part of the landward slope first decreased slightly and then remained stable. The three points at pressure gauge P7 from trial 22, trial 23, and trial 24 with a freeboard of -0.6 m tended to be greater than the average trend. Such deviation might be due to the effect of the combination of the downward-flushing flow impact and static pressure. A comparison of pressure gauges P6–P9 indicated that the values of a_{ps} had no apparent regularity during each test. The solid line is a best-fit empirical equation for the datasets given by the following equation:

$$a_{ps} = 22.3 \exp\left(-28.28 \frac{q_{ws}}{(gH_{m0}^3)^{0.5}}\right) + 0.65 \quad (10)$$

Figure 12 plots the shape factors b_{pc} on the dike crest and b_{ps} on the upper part of the landward slope versus the dimensionless overtopping discharge $[q_{ws}/m0_3^{*0.5}]$. It can be seen from Figure 12A that the shape factor b_{pc} on the dike crest increased with increasing $q_{ws}/m0_3^{*0.5}$. A comparison of pressure gauges P1–P5 indicated that the values of b_{pc} were nearly the same at these pressure gauges during each test. One data point at pressure gauge P3 from trial 25 tended to be greater than the average trend. Such deviation might be due to the H_{m0} ($H_{m0} = 1.51$ m) being relatively large in this test case. The solid line is the best-fit empirical equation for the datasets given by the following equation:

$$b_{pc} = 29.6 \frac{q_{ws}}{(gH_{m0}^3)^{0.5}} + 1.9 \quad (11)$$

It can be seen from Figure 12B that the shape factor b_{ps} on the upper part of the landward slope increased with increasing $q_{ws}/m0_3^{*0.5}$. A comparison of pressure gauges P6–P9 indicated that the values of b_{ps} were nearly the same at these pressure gauges during each test case. The solid line is the best-fit empirical equation for the datasets given by the following equation:

$$b_{ps} = 15.3 \frac{q_{ws}}{(gH_{m0}^3)^{0.5}} + 5.4 \quad (12)$$

The values of the scale factor a_p and the shape factor b_p can be used to calculate the maximum value of the Weibull distribution as (Pan et al., 2015):

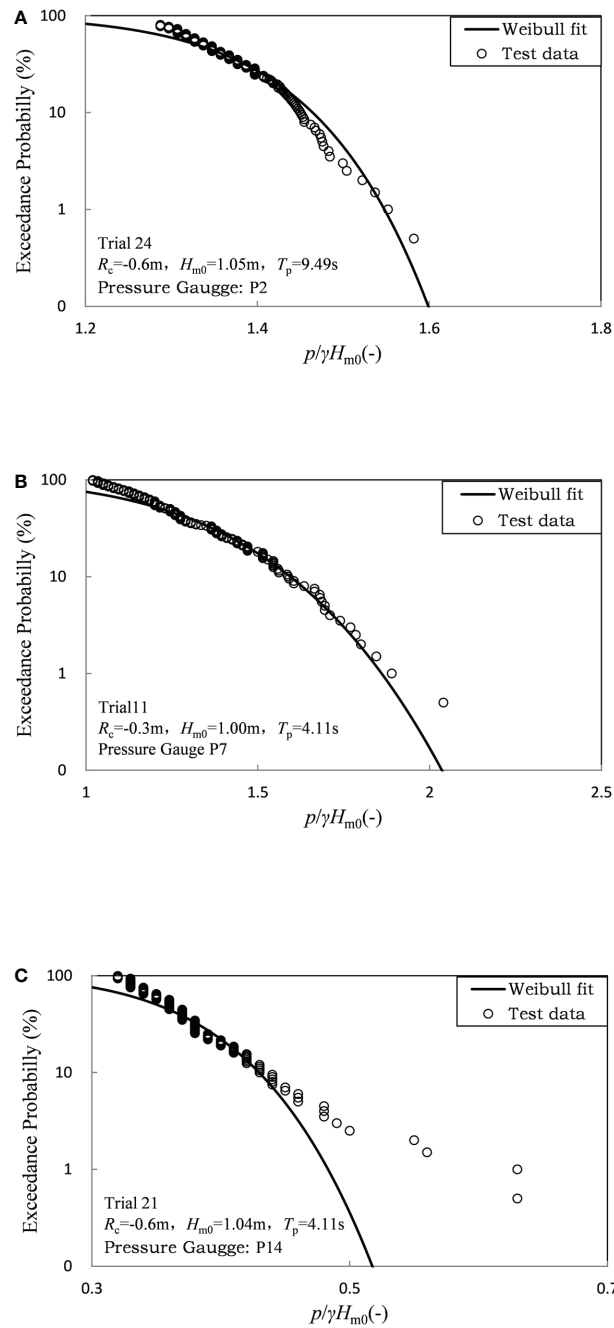
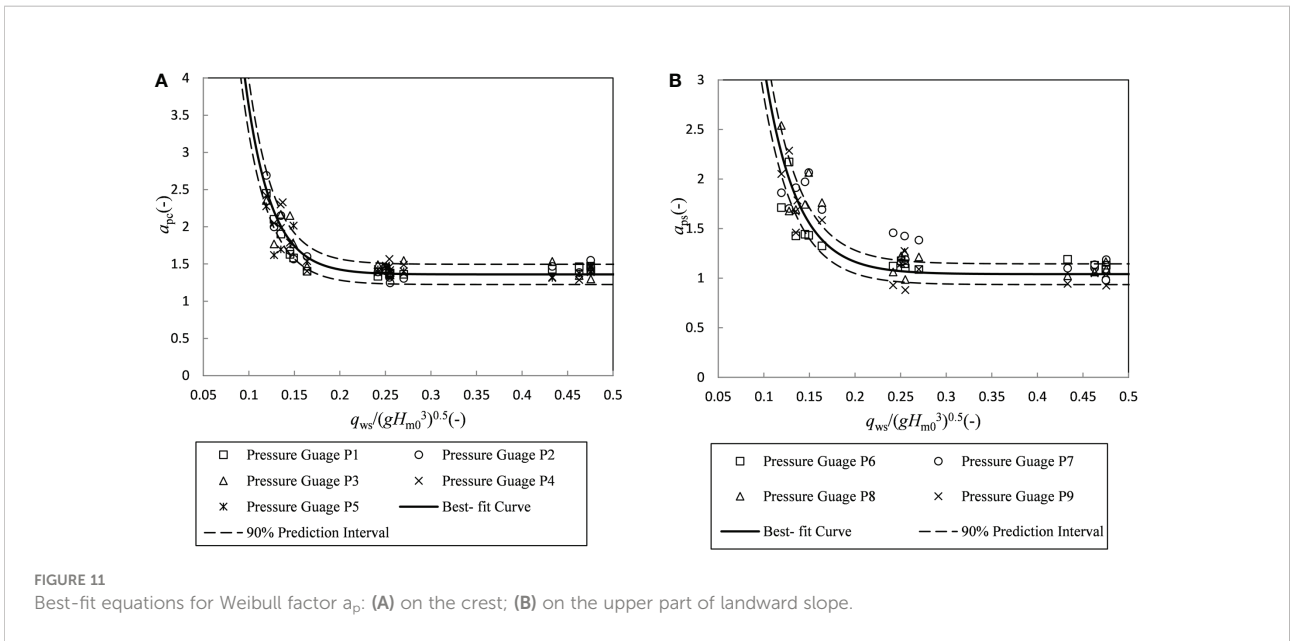


FIGURE 10
 Example of the best fits of the Weibull distribution to the peak value of normal stress. **(A)** Example of a mediocre fit from trial 21 (pressure gauge P2). **(B)** Example of a good fit from trial 11 (pressure gauge P7). **(C)** Example of a poor fit from trial 21 (pressure gauge P14).

$$p_{\max} = a_p (\ln(N + 1))^{1/b_p} \quad (13)$$

where N is the peak normal stress number. From Eqs. 9–12, the scale factor a_p and the shape factor b_p were calculated for all test cases. Then, Eq. 13 was used to estimate the maximum normal stress. Comparisons between the estimated and measured values

for the maximum normal stress on the dike crest and upper part of the landward slope are shown in Figure 13. A better prediction can be found for the maximum normal stress on the dike crest, as shown in Figure 13A. The estimation of maximum normal stress on the upper part of the landward slope was mediocre, but reasonable, as shown in Figure 13B. The data showed a good



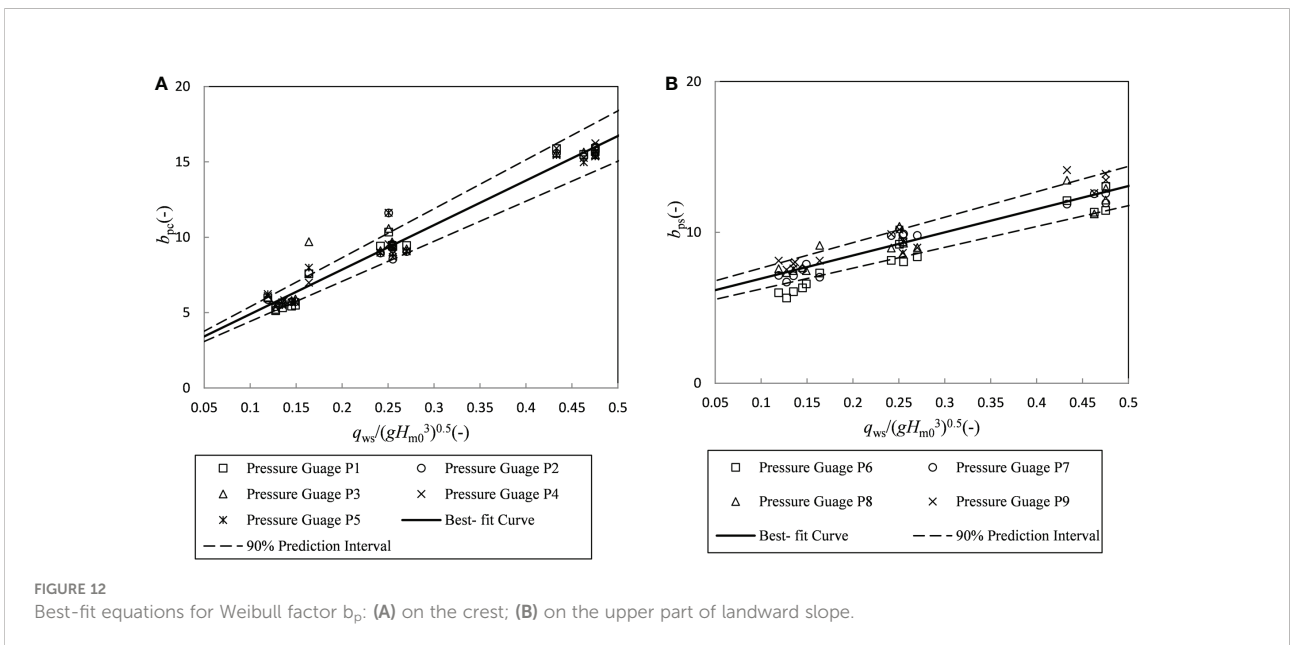
trend, but the data points were scattered because of the limited wave numbers and the randomness of the maximum value in limited cases.

5 Conclusions

this paper, the normal stress on a trapezoidal dike cross-section induced by the combined wave and surge overtopping was analyzed using laboratory measurements. The existing average overtopping discharge formulas were compared. The

characteristics of normal stress on the dike were obtained based on the analyses of the time series and spatial distribution of normal stress. Two empirical equations were proposed to represent the statistical distribution of peak normal stress. The main conclusions are discussed below.

For higher absolute values of relative freeboard ($R_c/H_{m0} < -0.4$), the average overtopping discharge of the combined wave and surge overtopping was close to the surge-only overflow discharge. For lower absolute values of relative freeboard, the average overtopping discharge of the combined wave and surge overtopping (q_{ws}) was slightly higher than the



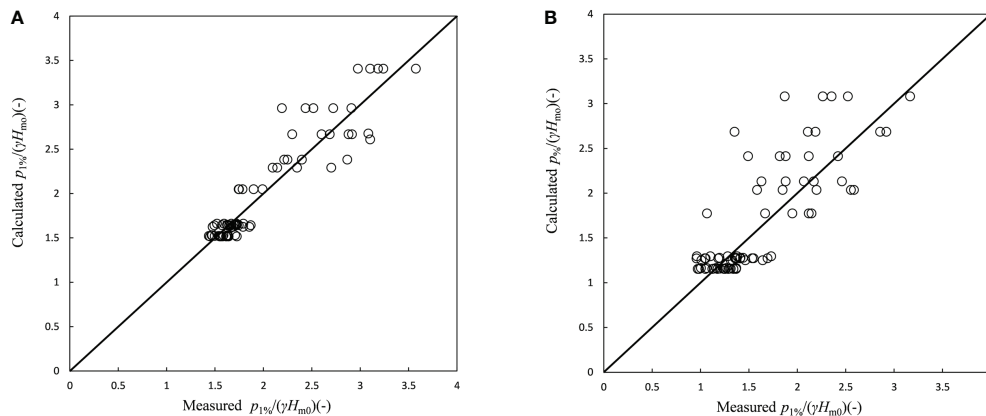


FIGURE 13

Comparison of measured and calculated maximum normal stress: (A) on the dike crest; (B) on the upper part of landward slope.

surge-only overflow discharge (q_s). Equation 7 (Hughes and Nadal, 2009) can be used to calculate the average discharge of the combined wave and surge overtopping in cases of higher absolute values of negative relative freeboard ($R_c/H_{m0} < -0.4$), while Eq. 1 (EurOtop, 2017) can be used to calculate the average discharge of the combined wave and surge overtopping in cases of lower absolute values of negative relative freeboard ($-0.4 \leq R_c/H_{m0} < 0$).

Two characteristics of normal stress can be observed during the tests: a) the abrupt change caused by the downward-flushing flow directly impacting the dike and b) the gradual change caused by the static pressure. In cases of lower absolute values of negative freeboard ($R_c = -0.3$ m), the normal stress on the dike was characterized by abrupt change. In cases of medium absolute values of negative freeboard ($R_c = -0.6$ m), the normal stress on dike crest ($0 \leq x/B < 1$) was characterized by gradual change, while the normal stress on the upper part of the landward slope ($1 \leq x/B < 2.1$) was characterized by abrupt change. Under higher absolute values of negative freeboard ($R_c = -0.9$ m), the normal stress on the dike was characterized by gradual change. Moreover, analysis of the spatial distribution of normal stress on the dike revealed that the normal stress occurring at the dike crest ($0 \leq x/B < 1$) and the upper part of the landward slope ($1 \leq x/B < 2.1$) was apparently larger than that occurring at the lower part of the landward slope ($x/B \geq 2.1$).

The two-parameter Weibull distribution shown by Eq. 8 was used to represent the statistical distribution of the peak normal stress. Equations 9, 11 described the calculations used to estimate the scale factor a_{pc} and the shape factor b_{pc} on the part of the dike crest. On the other hand, the calculations given in Eqs. 10, 12 were used to estimate the scale factor a_{ps} and the shape factor b_{ps} on the upper part of the landward slope. The maximum normal stress can be estimated using the calculated Weibull factors a_p and b_p . The calculated maximum normal stress on the

dike crest fitted the measurements well, while that on the upper part of the landward slope was mediocre, but was acceptable.

This paper provided better knowledge on the normal stress on dike induced by the combination of wave and surge overtopping. The conclusions presented in this paper are only suitable for dikes with a slope gradient of 1:4.25, and the equations may not be applicable for dikes with a different slope gradient.

Data availability statement

The original contributions presented in the study are included in the article/Supplementary Material. Further inquiries can be directed to the corresponding author.

Author contributions

ZZ: Conceptualization, methodology, software, writing—original draft, and writing—review and editing. ZS: Formal analysis, validation, visualization, and data curation. YZ: Writing—review and editing, and methodology. QZ and YC: Methodology. HW: Software. FH: Data curation. All authors contributed to the article and approved the submitted version.

Funding

We sincerely thank the fundings support from the National Natural Science Foundation of China (no. 51979098) and Fundamental Research Funds for Central Public Welfare Research Institutes (no. Y222010) and Jiangsu Funding Program for Excellent Postdoctoral Talent (no. 2022ZB10).

Conflict of interest

The authors declare that the research was conducted in the absence of any commercial or financial relationships that could be construed as a potential conflict of interest.

Publisher's note

All claims expressed in this article are solely those of the authors and do not necessarily represent those of their affiliated

organizations, or those of the publisher, the editors and the reviewers. Any product that may be evaluated in this article, or claim that may be made by its manufacturer, is not guaranteed or endorsed by the publisher.

Supplementary material

The Supplementary Material for this article can be found online at: <https://www.frontiersin.org/articles/10.3389/fmars.2022.1073345/full#supplementary-material>

References

- ASCE Hurricane Katrina External Review Panel (2007). *The new Orleans hurricane protection system: What went wrong and why?* (Reston, Virginia: American Society of Civil Engineers), 92.
- Celi, D., Pasquali, D., Fischione, P., Nucci, C., and Risio, M. (2021). Wave-induced dynamic pressure under rubble mound breakwaters with submerged berm: An experimental and numerical study. *Coast. Eng.* 170, 104014. doi: 10.1016/j.coastaleng.2021.104014
- EurOtop (2017). Manual on wave overtopping of sea defences and related structure. *An overtopping manual largely based on European research, but for worldwide application.* J. W. Van der Meer, N. W.H. Allsop, T. Bruce, J. De Rouck, A. Kortenhaus, T. Pullen, et al. Available at: www.overtopping-manual.com.
- Hattori, M., Arami, A., and Yui, T. (1994). Wave impact pressure on vertical walls under breaking waves of various types. *Coast. Eng.* 22, 79–114. doi: 10.1016/0378-3839(94)90049-3
- Henderson, F. M. (1966). *Open channel flow* (New York: MacMillan Publishing Co.).
- Hughes, S. A. (2008). "Levee overtopping design guidance: what we know and what we need," in *Proceedings of the solutions to coastal disasters congress* (Turtle Bay, Oahu, Hawaii: ASCE), 867–880.
- Hughes, S. A., and Nadal, N. C. (2009). Laboratory study of combined wave overtopping and storm surge overflow of a levee. *Coast. Eng.* 56 (2009), 244–259. doi: 10.1016/j.coastaleng.2008.09.005
- Hughes, S. A., Shaw, J. M., and Howard, I. L. (2011). Earthen levee shear stress estimates for combined wave overtopping and surge overflow. *J. Wat Port Coast. Ocean Eng.* ASCE 138 (3), 267–273. doi: 10.13140/RG.2.2.21298.63681
- IPCC (2012). "Managing the risks of extreme events and disasters to advance climate change adaptation," in *A special report of working Groups I and II of the intergovernmental panel on climate Chang* (Cambridge, UK, and New York, NY, USA: Cambridge University Press), 582p.
- Jensen, B., Christensen, E. D., and Mutlu Sumer, B. (2014). Pressure-induced forces and shear stresses on rubble mound breakwater armour layers in regular waves. *Coast. Eng.* 91, 60–75. doi: 10.1016/j.coastaleng.2014.05.003
- Li, L., Pan, Y., Amini, F., and Kuang, C. P. (2012). Full scale laboratory study of combined wave and surge overtopping of a levee with RCC strengthening system. *Ocean Eng.* 54 (1), 70–86. doi: 10.1016/j.oceaneng.2012.07.021
- Pan, Y., Kuang, C. P., Li, L., and Amini, F. (2015). Full-scale laboratory study on distribution of individual wave overtopping volumes over a levee under negative freeboard. *Coast. Eng.* 97, 11–20. doi: 10.1016/j.coastaleng.2014.12.007
- Pan, Y., Li, L., Amini, F., and Kuang, C. (2012). Full scale HPTRM strengthened levee testing under combined wave and surge overtopping conditions: Overtopping hydraulics, shear stress and erosion analysis. *J. Coast. Res.* 29 (1), 182–200. doi: 10.2112/JCOASTRES-D-12-00010.1
- Pan, Y., Li, L., Amini, F., and Kuang, C. P. (2013a). Full-scale HPTRM-strengthened levee testing under combined wave and surge overtopping conditions: overtopping hydraulics, shear stress, and erosion analysis. *J. Coast. Res.* 29 (1), 182–200. doi: 10.2112/JCOASTRES-D-12-00010.1
- Pan, Y., Li, L., Amini, F., and Kuang, C. P. (2013b). Influence of three levee-strengthening systems on overtopping hydraulic parameters and hydraulic equivalency analysis between steady and intermittent overtopping. *J. Wat Port Coast. Ocean Eng.* 139 (4), 256–266. doi: 10.1061/(ASCE)WW.1943-5460.0000179
- Pan, Y., Yin, S., Chen, Y. P., Yang, Y. B., Xu, C. Y., and Xu, Z. S. (2022). An experimental study on the evolution of a shoreface nourishment under the effects of regular waves in low-energy conditions. *Coast. Eng.* 176, 104169. doi: 10.1016/j.coastaleng.2022.104169
- Pan, Y., Zhou, Z. J., and Chen, Y. P. (2020). An analysis of the downward-flushing flow on the crest of a levee under combined wave and surge overtopping. *Coast. Eng.* 158, 103701. doi: 10.1016/j.coastaleng.2020.103701
- Raby, A., Bullock, G., Jonathan, P., Randell, D., and Whittaker, C. (2022). On wave impact pressure variability. *Coast. Eng.* 177, 104168. doi: 10.1016/j.coastaleng.2022.104168
- Reeve, D. E., Soliman, A., and Lin, P. Z. (2008). Numerical study of combined overflow and wave overtopping over a smooth impermeable seawall. *Coast. Eng.* 55 (2), 155–166. doi: 10.1016/j.coastaleng.2007.09.008
- Schüttrumpf, H., Möller, J., Oumeraci, H., Grüne, J., and Weissmann, R. (2005). Effects of natural sea states on wave overtopping of sea dikes [C]. *Proceedings Waves 2001, Conference*, 1565–1574.
- Yuan, S. Y., Li, L., Amini, F., and Tang, H. W. (2014). Turbulence measurement of combined wave and surge overtopping over a full scale HPTRM strengthened levee. *J. Wat Coast. Ocean Eng.* 140, 04014014. doi: 10.1061/(ASCE)WW.1943-5460.0000230
- Zhou, Z. J., Chen, Y. P., Pan, Y., Shen, Y. S., and Gan, M. (2020). Wave-induced uplift pressure on berm revetment with seabee slope. *Coast. Eng. J* 62 (4), 527–539. doi: 10.1080/21664250.2020.1816527